

Measurement of τ branching ratios

H. Aihara,ⁿ M. Alston-Garnjost,^a R. E. Avery,^a J. A. Bakken,^j A. Barbaro-Galtieri,^a
 A. R. Barker,^g A. V. Barnes,^a B. A. Barnett,^j D. A. Bauer,^g H.-U. Bengtsson,^d
 D. L. Bintinger,^f B. J. Blumenfeld,^j G. J. Bobbink,^h T. S. Bolognese,^a A. D. Bross,^a
 C. D. Buchanan,^d A. Buijs,^m D. O. Caldwell,^g C.-Y. Chien,^j A. R. Clark,^a G. D. Cowan,^a
 D. A. Crane,^j O. I. Dahl,^a K. A. Derby,^a J. J. Eastman,^a T. K. Edberg,^a P. H. Eberhard,^a
 A. M. Eisner,^c R. Enomoto,ⁿ F. C. Ern ,^m T. Fujii,ⁿ J. W. Gary,^a W. Gorn,^c
 J. M. Hauptman,ⁱ W. Hofmann,^a J. E. Huth,^a J. Huyen,^j T. Kamae,ⁿ H. S. Kaye,^a
 K. H. Kees,^f R. W. Kenney,^a L. T. Kerth,^a Winston Ko,^b R. I. Koda,^d R. R. Kofler,^k
 K. K. Kwong,^c R. L. Lander,^b W. G. J. Langeveld,^e J. G. Layter,^c F. L. Linde,^m
 C. S. Lindsey,^c S. C. Loken,^a A. Lu,^g X.-Q. Lu,^j G. R. Lynch,^a L. Madansky,^j
 R. J. Madaras,^a K. Maeshima,^b B. D. Magnuson,^c J. N. Marx,^a G. E. Masek,^f L. G. Mathis,^a
 J. A. J. Matthews,^j S. J. Maxfield,^k S. O. Melnikoff,^c E. S. Miller,^f W. Moses,^a
 R. R. McNeil,^b P. Nemethy,^l D. R. Nygren,^a P. J. Oddone,^a H. P. Paar,^m D. A. Park,^d
 S. K. Park,ⁱ D. E. Pellett,^b A. Pevsner,^j M. Pripstein,^a M. T. Ronan,^a R. R. Ross,^a
 F. R. Rouse,^a K. A. Schwitkis,^g J. C. Sens,^m G. Shapiro,^a M. D. Shapiro,^a B. C. Shen,^c
 W. E. Slater,^d J. R. Smith,^b J. S. Steinman,^d M. L. Stevenson,^a D. H. Stork,^d
 M. G. Strauss,^d M. K. Sullivan,^c T. Takahashi,ⁿ J. R. Thompson,^f N. Toge,ⁿ
 S. Toutouchi,^k R. van Tyen,^a B. van Uiter,^m G. J. VanDalen,^c
 R. F. van Daalen Wetters,^d W. Vernon,^f W. Wagner,^b E. M. Wang,^a Y. X. Wang,^g M. R. Wayne,^d
 W. A. Wenzel,^a J. T. White,^f M. C. S. Williams,^b Z. R. Wolf,^a H. Yamamoto,^a S. J. Yellin,^g
 C. Zeitlin,^b and W.-M. Zhang^j

^aLawrence Berkeley Laboratory, Berkeley, California 94720

^bUniversity of California, Davis, California 95616

^cUniversity of California Institute for Research at Particle Accelerators, Stanford, California 94305

^dUniversity of California, Los Angeles California 90024

^eUniversity of California, Riverside, California 92521

^fUniversity of California, San Diego, California 92093

^gUniversity of California, Santa Barbara, California 93106

^hCarnegie-Mellon University, Pittsburgh, Pennsylvania 15213

ⁱAmes Laboratory, Iowa State University, Ames, Iowa 50011

^jJohns Hopkins University, Baltimore, Maryland 21218

^kUniversity of Massachusetts, Amherst, Massachusetts 01003

^lNew York University, New York, New York 10003

^mNational Institute for Nuclear and High Energy Physics, Amsterdam, The Netherlands

ⁿUniversity of Tokyo, Tokyo, Japan

(TPC/Two-Gamma Collaboration)

(Received 14 October 1986)

We have measured the branching ratios for several τ decay modes. We use $e^+e^- \rightarrow \tau^+\tau^-$ events accumulated with the TPC/Two-Gamma facility at the SLAC e^+e^- storage ring PEP. The data correspond to an integrated luminosity of 77 pb^{-1} at a center-of-mass energy of 29 GeV. The one- and three-charged-particle inclusive branching ratios of the τ decay are measured to be $B_1 = (84.7 \pm 1.0)\%$ and $B_3 = (15.1 \pm 1.0)\%$, where $B_1 + B_3$ is constrained to be 99.85%. The branching ratios of the two leptonic decay modes are $B(\tau^- \rightarrow e^- \bar{\nu}_e \nu_\tau) = (18.4 \pm 1.6)\%$ and $B(\tau^- \rightarrow \mu^- \bar{\nu}_\mu \nu_\tau) = (17.7 \pm 1.4)\%$. If we then assume lepton universality, we obtain $B(\tau^- \rightarrow e^- \bar{\nu}_e \nu_\tau) = (18.3 \pm 0.9)\%$ and $B(\tau^- \rightarrow \mu^- \bar{\nu}_\mu \nu_\tau) = (17.8 \pm 0.9)\%$. We measure the Cabibbo-allowed semihadronic decay mode $B(\tau^- \rightarrow \pi^- + \text{neutral particles}) = (47.0 \pm 1.5)\%$, and the Cabibbo-suppressed τ decay mode $B(\tau^- \rightarrow K^- + \text{neutral particles}) = (1.6 \pm 0.4)\%$. By looking for associated photons, we find $B(\tau^- \rightarrow K^- \pi^0 + \text{neutral particles})$ to be $(1.2 \pm 0.6)\%$. Using the channel $K^{*-} \rightarrow K_S^0 \pi^- \rightarrow \pi^+ \pi^- \pi^-$, we find $B(\tau^- \rightarrow K^{*-} (892) + \text{neutral particles}) = (1.4 \pm 0.9)\%$. The quoted errors are the combined statistical and systematic errors.

I. INTRODUCTION

Measurement of τ lepton decay branching ratios provide many tests of the weak interaction, including tests of lepton universality, CVC (conservation of vector current), PCAC (partial conservation of axial-vector current), and our general understanding of the hadronic weak interactions. All measurements of individual branching ratios made thus far are consistent with expectations from theory. However, the most recent theoretical estimation of the sum of the modes contributing to the topological one-charged-particle branching ratio¹ is significantly less than the measured topological one-charged-particle branching ratio. Additional measurements of the main τ decay modes are thus useful to help determine if the effect seen is only a statistical fluctuation. Measurement of the Cabibbo-suppressed τ decay modes involving strange mesons are of special significance in that they may be especially sensitive to any unexpected interactions.

In this paper we report the measurement of branching ratios of two leptonic τ decay modes:

$$B_e \equiv B(\tau^- \rightarrow e^- \bar{\nu}_e \nu_\tau),$$

and

$$B_\mu \equiv B(\tau^- \rightarrow \mu^- \bar{\nu}_\mu \nu_\tau);$$

and semihadronic decay modes:

$$B_h \equiv B(\tau^- \rightarrow \text{one charged hadron} + \text{neutral particles})$$

and

$$B_\pi \equiv B(\tau^- \rightarrow \pi^- + \text{neutral particles});$$

and two topological decay modes:

$$B_1 \equiv B(\tau^- \rightarrow \text{one charged prong} + \text{neutral particles})$$

and

$$B_3 \equiv B(\tau^- \rightarrow \text{three charged prongs} + \text{neutral particles});$$

as well as three Cabibbo-suppressed τ decay modes:

$$B_K \equiv B(\tau^- \rightarrow K^- + \text{neutral particles}),$$

$$B_{K\pi^0} \equiv B(\tau^- \rightarrow K^- + \pi^0 + \text{neutral particles}),$$

and

$$B_{K^*} \equiv B(\tau^- \rightarrow K^{*-}(892) + \text{neutral particles}).$$

The general outline of this paper is as follows. First we briefly describe the experimental apparatus used. Then we list the topological and kinematic cuts used to select $\tau\tau \rightarrow (\text{one-charged-prong} + \text{one-charged-prong})$ and $\tau\tau \rightarrow (\text{one-charged-prong} + \text{three-charged-prong})$ events. We follow this with a description of the particle identification used to separate the leptonic and inclusive semihadronic modes. We then describe the measurement of the Cabibbo-suppressed modes. We end with a discussion of our results.

II. APPARATUS

The data were taken with the TPC/Two-Gamma facility at the Stanford Linear Accelerator Center storage ring PEP. This facility and all its elements have been described in detail elsewhere.² The present analysis made use of identification of photons, muons, electrons, and charged pions and kaons. Charged particles were identified in the time projection chamber (TPC), a drift chamber that simultaneously measures their momentum and dE/dx energy loss. The momentum resolution was typically

$$\delta P/P = [(0.06)^2 + (0.035P)^2]^{1/2}$$

with P in GeV/ c . The dE/dx measurement made by sampling the ionization up to 183 times had a resolution of 3.7%. Because muons and pions have similar dE/dx , muons had to be identified by detection in drift chambers interleaved with iron hadron absorber. These “muon chambers” had four layers in the central region and three layers in the forward-backward region, with a fiducial coverage for this analysis of 76% of 4π . The detection efficiency of muon chambers was more than 98% for muons with a momentum above 2 GeV/ c . Photons were either detected in the hexagonal calorimeter (HEX) or reconstructed from an e^+e^- conversion pair by the TPC. The HEX was a gas Pb-laminate sampling calorimeter 10-radiation-length-thick run in limited Geiger mode. Its single-photon energy resolution was $16\%/\sqrt{E}$ with E in GeV, and it had an effective coverage of 59% of 4π for this analysis. The data used for this analysis correspond to an integrated luminosity of $77 \pm 5 \text{ pb}^{-1}$ at a center-of-mass energy of 29 GeV.

III. $\tau\tau$ EVENT SELECTION

Two data samples of $e^+e^- \rightarrow \tau^+\tau^-$ events were selected using mainly topological and kinematic cuts. One data sample consisted of $\tau(1+3)$ events which had final-state topologies containing one charged particle opposite to three charged particles, while the other consisted of $\tau(1+1)$ events in which each τ decayed to only one charged particle.

For use in suppressing electron backgrounds, we formed χ_e^2 using the difference between the measured dE/dx for a given track and the expected dE/dx for an electron at that track's momentum. We defined $(\chi_{\min(\mu,\pi,K)})^2$ as the smallest of the χ^2 's for that track found using the dE/dx expected for a muon, a pion, and a kaon. A track was then classed as “likely to be an electron” if $\chi_e^2 < 9$ and $(\chi_{\min(\mu,\pi,K)})^2 > 9$. A track was classed as a “nonelectron” if $\chi_e^2 > (\chi_{\min(\mu,\pi,K)})^2 + 3$ and $(\chi_{\min(\mu,\pi,K)})^2 < 7$.

In selecting $\tau(1+3)$ events, it was necessary to allow for extra pairs of e^+e^- tracks from photon conversions and to impose cuts beyond simple topology to suppress backgrounds. The $\tau(1+3)$ selection requirements were the following.

(1) The event had exactly four good charged tracks, where a good track had (a) momentum $> 300 \text{ MeV}/c$, (b) angle from the beam $> 30^\circ$, (c) an extrapolated orbit

within 10 cm of the nominal interaction point in the beam direction and 5 cm in the plane perpendicular to the beams, and (d) not been geometrically reconstructed as part of an e^+e^- photon conversion pair.

(2) The total charge of the four tracks was equal to zero.

(3) One track (called the “isolated” track) was $> 140^\circ$ from each of the other three tracks.

(4) The invariant mass of the three nonisolated tracks was $< 2 \text{ GeV}/c^2$ (assuming pion rest masses).

(5) The scalar sum of the total visible charged momenta was (a) $> 4.5 \text{ GeV}/c$ and (b) $< 24.0 \text{ GeV}/c$.

(6) The nonisolated tracks were not “likely electrons.”

(7) The angle between the highest-momentum track and any of the other three tracks was $< 178^\circ$.

Criteria (1), (2), and (3) selected the $\tau(1+3)$ topology. Background from multihadron events was reduced by the invariant-mass criterion (4) and the momentum-sum criterion (5b). Radiative Bhabha and μ -pair events were reduced by the dE/dx criterion (6) and the acollinearity criterion (7). Background from two-photon and beam gas events was reduced by the topological criterion (3) and the momentum-sum criterion (5a). Unreconstructed photon-conversion pairs were reduced by the dE/dx criterion (6). Note that $\pi^+\pi^-$ from K_S^0 which decay close to the interaction point were not excluded in the three-prong selection. With these criteria, we found 660 $\tau(1+3)$ candidates.

For the $\tau(1+1)$ sample, we used tight track cuts to select events with single prongs in opposite hemispheres (allowing for accompanying photon-conversion pairs and δ rays), but vetoed the event if additional tracks were found when the track cuts were loosened. The tight (loose) track-selection criteria were (i) the momentum was ≥ 300 (100) MeV/c , (ii) the angle θ with respect to the beam line was $\geq 35^\circ$ (20°), and (iii) the extrapolated orbit passed the nominal interaction point within 5 (10) cm along the beam line and within 2 (5) cm in the plane perpendicular to the beam line. The criteria for a $\tau(1+1)$ event were then as follows.

(1) There was exactly one acollinear pair of candidate tracks with opposite charge in the event. The remaining tracks were either “likely electrons” as determined by dE/dx analysis or part of geometrically reconstructed photon conversions. Specifically, the two candidate tracks in the selected pair satisfied the criteria that (a)

their acollinearity angle was between 3° and 55° , (b) their acoplanarity (using the beam axis) was between 1° and 55° , and (c) neither was identified as part of a photon conversion pair.

(2) At least one of the two tracks in the acollinear pair was identified as a “nonelectron.” If only one of them was so identified, the momentum of this track was required to be $\leq 9.5 \text{ GeV}/c$.

(3) The scalar sum of the visible charged momenta was between 7.25 and 22 GeV/c .

(4) The sphericity of the event was ≤ 0.06 .

(5) The scalar sum of the momenta of the tracks in each of two hemispheres (defined by a plane perpendicular to the sphericity axis) was $\geq 0.65 \text{ GeV}/c$.

Criterion (1) defined the topology of $\tau(1+1)$ events, where the acollinearity criterion eliminated background from radiative Bhabha and μ -pair events, and requiring exactly one acollinear pair reduced contamination from multihadron and $\tau(1+3)$ events. The nonelectron criterion (2) was necessary to reduce further the contamination from radiative Bhabha events. The momentum sum criterion (3) and sphericity criterion (4) eliminated background from two-photon, radiative Bhabha, radiative μ -pair, and multihadron events. The one side momentum-sum criterion (5) rejected beam-gas events.

A total of 1493 $\tau(1+1)$ event candidates were selected with the above criteria. This included events taken with a charged-particle trigger,³ a neutral-energy trigger, and a charged-neutral combined trigger. In order to simplify the estimation of the trigger efficiency, and thereby reduce systematic errors, only the 1178 events from the charged-particle trigger were used to calculate branching ratios.

IV. PARTICLE IDENTIFICATION

The single prong τ decays were then classified by particle type using the muon system and dE/dx particle identification. To be classified using the muon system, a track had to satisfy the following fiducial cuts: (i) angle with respect to the beam axis between 30° and 50° or between 57.3° and 90° and (ii) momentum greater than 2 GeV/c . To be classified using the dE/dx system, a track had to have a well-measured dE/dx as defined by (i) the track had to have at least 80 measured dE/dx samples, (ii) it was not near the boundaries of the TPC end-cap sectors,

TABLE I. Summary of the $\tau(1+3)$ event categorization.

Category	Momentum range (GeV/c)	Identification of the isolated track	
		Polar angular region	Identified by
μ -3	≥ 2	$30^\circ-50^\circ, 57.3^\circ-90^\circ$	Muon system
e -3	$0.3-2$	$30^\circ-50^\circ, 57.3^\circ-90^\circ$	dE/dx
h -3	≥ 2	$30^\circ-50^\circ, 57.3^\circ-90^\circ$	Muon system veto and dE/dx
(μ/h) -3	≥ 2	$50^\circ-57.3^\circ$	Muon system veto and dE/dx
	≥ 2	$50^\circ-57.3^\circ$	dE/dx
	$0.3-2$	$30^\circ-90^\circ$	dE/dx
Miscellaneous $\tau(1+3)$	Not able to classify the track in any of the above categories		

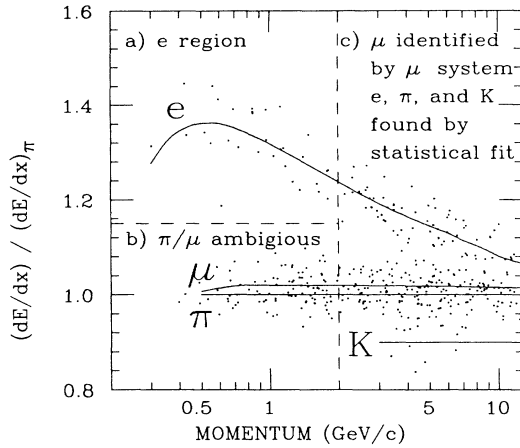


FIG. 1. dE/dx , normalized to the dE/dx expected for a pion, vs momentum for all one-prongs in the $\tau(1+3)$ sample which had a well-measured dE/dx . The curves denote the expected dE/dx for electrons, muons, pions, and kaons, respectively. Indicated also are the different sample selection regions.

and (iii) its momentum was < 12.8 GeV/ c , since particle identification at higher momentum was limited by the momentum resolution.

The 660 $\tau(1+3)$ events were divided into five categories, μ -3, e -3, h -3, (μ/h) -3, and miscellaneous $\tau(1+3)$, according to how well our particle-identification systems could identify the isolated track. In the first three categories the isolated track was identified as a muon, electron, or hadron. To be in the fourth category, (μ/h) -3, the isolated track was identified as a nonelectron by dE/dx , but its identity was ambiguous between either the muon or hadron because the track was outside the muon system fiducial cuts. The miscellaneous category consisted of all $\tau(1+3)$ events not in the above four categories, that is, those events with isolated tracks which were not identified as muons and which did not have well-measured dE/dx . Table I summarizes the identification systems and fiducial cuts used for each sample. Figure 1 shows the dE/dx of the isolated tracks (normalized to the dE/dx expected for a pion) versus momentum. The sample regions are also indicated on this plot, along

with curves for dE/dx expected for electrons, muons, pions, and kaons.

The separation of the $\tau(1+3)$ events into the five categories was specifically performed as follows.

(1) Of the events with isolated tracks satisfying the muon system fiducial cuts (region c in Fig. 1), (a) 89 were identified by the muon system as μ -3 candidates and (b) 273 had isolated tracks which were identified as nonmuons and also had well-measured dE/dx , from which a fit to the dE/dx distribution gave 76.7 ± 9.2 e -3 and 196.3 ± 14.6 h -3 candidates.

(2) Of the events with isolated tracks not satisfying the muon system fiducial cuts but with well-measured dE/dx , (a) 32 had isolated tracks with momentum less than 2 GeV/ c and dE/dx more than 4 standard deviations larger than that expected for pions and muons (region a in Fig. 1) and were added to the e -3 candidates and (b) the rest were statistically fit to remove electrons, which gave 162.3 ± 13.8 (μ/h) -3 candidates (region b in Fig. 1, and some tracks in region c which were outside the muon system angular coverage).

(3) The 103.7 ± 12.5 events not selected in the previous categories were classed as miscellaneous $\tau(1+3)$ candidates.

Four categories of events, h - h , e - μ , h - μ , and (μ/h) - h , were selected from the $\tau(1+1)$ sample according to the identity of each of the two tracks in the acollinear pair in the event. Events of the type μ - μ , μ - (μ/h) , etc., were not used in the analysis because of the large background from $\tau\tau \rightarrow \mu\mu\gamma$, and events of the type e - e , e - h , etc., were not used because of radiative Bhabha contamination. The selection of the four categories is summarized in Table II, and specifically proceeded as follows.

(1) 146 events were selected as h - h event candidates by requiring that (a) both the tracks in the acollinear pair were identified as "nonelectrons" by dE/dx and (b) both satisfied the muon system fiducial cuts and were identified as nonmuons.

(2) A set of e - μ and h - μ event candidates were initially selected together by requiring that (a) both tracks satisfied the muon system fiducial cuts, (b) exactly one of them was identified as a muon, and (c) the other track had well-measured dE/dx .

Then, 42.8 ± 7.1 and 151.2 ± 12.7 events were identified

TABLE II. Summary of the $\tau(1+1)$ event categorization.

Category	Track	Identification of two tracks in the pair		
		Momentum range (GeV/ c)	Polar angular region	Identified by
h - h	Both	≥ 2	35° - $50^\circ, 57.3^\circ$ - 90°	Muon system veto and dE/dx
e - μ	μ	≥ 2	35° - $50^\circ, 57.3^\circ$ - 90°	Muon system
	e	0.3-2	35° - $50^\circ, 57.3^\circ$ - 90°	dE/dx
h - μ	μ	≥ 2	35° - $50^\circ, 57.3^\circ$ - 90°	Muon system veto and dE/dx
	Hadron	≥ 2	35° - $50^\circ, 57.3^\circ$ - 90°	Muon system
(μ/h) - h	Hadron	≥ 2	35° - $50^\circ, 57.3^\circ$ - 90°	Muon system veto and dE/dx
	μ /hadron	≥ 2	50° - 57.3°	dE/dx
		0.3-2	35° - 90°	dE/dx

TABLE III. Background contributions to the five $\tau(1+3)$ categories.

Background	Category				
	μ -3	e -3	h -3	(μ/h) -3	Miscellaneous-3
Multihadron	0.7±0.6	0.3±0.3	9.1±1.8	5.4±1.4	5.1±1.4
Bhabha		1.6±1.6			3.2±2.3
$e^+e^- \rightarrow e^+e^-q\bar{q}$		1.0±1.0			0.9±0.9
$e^+e^- \rightarrow e^+e^-\tau^+\tau^-$	0.8±0.5	1.9±0.8	3.1±1.1	1.5±0.8	1.9±0.8
$\tau(1+1)$	1.1±1.1		7.3±2.8	2.1±1.5	2.1±1.5
$\tau(3+3)$			1.6±0.9	1.0±0.8	1.1±0.8
Total	2.6±1.3	4.8±2.1	21.1±3.6	10.0±2.3	14.3±3.4

as e - μ and h - μ candidates by a statistical fit to the dE/dx distribution of the nonmuon tracks.

(3) A set of 9 events were added to the e - μ category which satisfied (a) one track satisfied the muon system fiducial cuts and was identified as a muon and (b) the momentum of the other tracks was < 2 GeV/ c and its dE/dx was at least 4 standard deviations larger than the expected value for pions or muons.

(4) From the remaining unclassified events, 185 (μ/h) - h event candidates were selected with the following selection criteria: (a) both of the tracks were identified as "nonelectrons," (b) one track satisfied the muon system fiducial cuts and was identified as a nonmuon, and (c) the other track did not satisfy the muon system fiducial cuts.

V. CORRECTIONS TO THE DATA

We applied corrections to each of these categories of events for trigger efficiency, geometrical reconstruction and selection efficiency, background contamination, and muon-hadron misidentification.

The trigger efficiency was estimated using a trigger Monte Carlo simulation that had been tuned using Bhabha and two-photon data. The trigger efficiency ranged from 57 to 96 % depending on the event type, the number of reconstructed tracks, and the orientation of the two tracks in the acollinear pair. This simulation was checked with real $\tau(1+1)$ and $\tau(1+3)$ events that had a neutral-energy trigger. The charged-particle trigger efficiency, calculated as the fraction of these events which also gave a charged-particle trigger, was checked in five angular regions and subdivided according to the number of reconstructed tracks. The Monte Carlo trigger efficiencies agreed with these measurements. The Monte Carlo trigger efficiencies were applied to each category of events according to angle and number of reconstructed tracks.

The geometric reconstruction and selection efficiency for events in each of the five $\tau(1+3)$ and four $\tau(1+1)$ categories was also estimated using a Monte Carlo simulation. This simulation modeled $\tau^+\tau^-$ pair production with a QED cross section⁴ accurate up to third order in α and τ decay with a statistical model⁵ adjusted to agree with published branching ratios.⁶ It included a full detector simulation.

The background contamination to events in each

category was estimated using a Monte Carlo simulation for various background sources: multihadron,⁵ radiative Bhabha, μ pair, two-photon events,⁷ and contamination from other τ decay channels. The various background contributions are listed in Tables III and IV.

A correction was made for hadrons that penetrated the iron absorber and were misidentified as muons. The misidentification probability in the central muon chambers for pions was estimated as a function of angle and momentum using a Monte Carlo simulation.⁸ For the forward-backward muon chambers, the misidentification probability for pions was estimated by taking the ratio of fake muons in hadrons from three-charged-prong τ decays in the $\tau(1+3)$ sample. The "muons" in the three-charged-prong decays were also used as a check of the Monte Carlo in the central muon chambers. Averaged over the momentum and angular spectrum of one-prong pions from τ decay, the misidentification probability was $(2.4 \pm 0.5)\%$.

Table V gives a summary of the number of selected events and the corrections and acceptances for each category.

VI. TOPOLOGICAL AND LEPTONIC BRANCHING RATIOS

A simultaneous χ^2 fit was made to the numbers of events in the nine categories to determine the branching ratios B_e , B_μ , B_h , $B_1(\equiv B_e + B_\mu + B_h)$, and B_3 . The expected number of events for each of the nine categories was calculated using the integrated luminosity, the $\tau\tau$ production cross section, and the appropriate branching ra-

TABLE IV. Background contributions to the four $\tau(1+1)$ categories.

Background	Category			
	h - h	e - μ	h - μ	(μ/h) - h
Multihadron				3.5±1.9
$e^+e^- \rightarrow e^+e^-\tau^+\tau^-$	0.5±0.4		1.1±0.5	1.1±0.6
$\tau(1+3)$	1.5±1.1			6.2±2.2
e - h	3.7±0.7			1.9±0.5
Total	5.7±1.5		1.1±0.5	12.7±2.9

tios and efficiencies. B_1+B_3 was constrained to be 99.85%, allowing for the measured 0.15% τ five-prong branching ratio.⁹⁻¹¹ A preliminary fit to the nine categories with the luminosity as a free parameter gave a luminosity of $79\pm 3(\text{stat})\text{ pb}^{-1}$, in good agreement with the luminosity of $77\pm 5\text{ pb}^{-1}$ measured with wide-angle Bhabha-scattering events. With the luminosity from the Bhabha measurement then also used as input to the fit, we found $B_e=(18.4\pm 1.2\pm 1.0)\%$, $B_\mu=(17.7\pm 1.2\pm 0.7)\%$, $B_h=(48.6\pm 1.2\pm 0.9)\%$, $B_1=(84.7\pm 0.8\pm 0.6)\%$, and $B_3=(15.1\pm 0.8\pm 0.6)\%$ (Ref. 12). The first error in these branching ratios is statistical and the second is systematic, where the systematic error reflects the uncertainty in the selection efficiency, the trigger efficiency, and the luminosity. The ratio of B_μ/B_e is 0.97 ± 0.13 as compared to 0.97 expected from lepton universality. If we assumed lepton universality and refit with this ratio fixed, we obtained $B_e=(18.3\pm 0.7\pm 0.5)\%$, or equivalently $B_\mu=(17.8\pm 0.7\pm 0.5)\%$, where B_h , B_1 , and B_3 did not change.

VII. $B(\tau^- \rightarrow K^- + \text{NEUTRAL PARTICLES})$

The branching ratio $B_K \equiv B(\tau^- \rightarrow K^- + \text{neutral particles})$ was measured using single-prong τ decays from both the $\tau(1+3)$ and $\tau(1+1)$ samples. Tracks were selected which had well-measured dE/dx as defined previously,

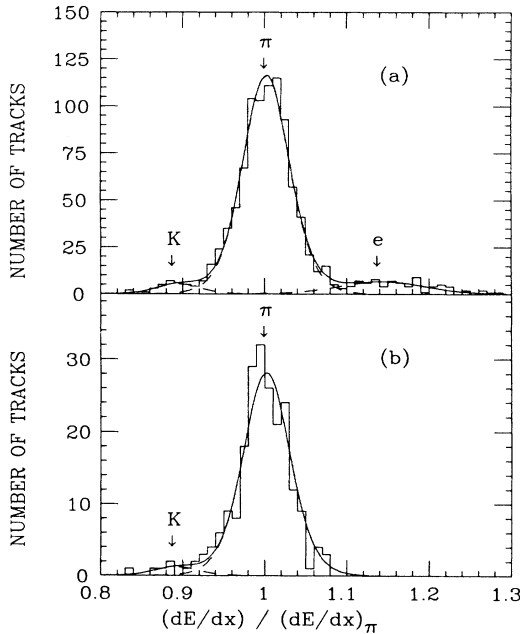


FIG. 2. The distribution of the dE/dx , normalized to the expected dE/dx for pions, for (a) all nonmuon tracks selected from both $\tau(1+3)$ and $\tau(1+1)$ samples with good dE/dx and $P \geq 2\text{ GeV}/c$ and (b) hadron tracks having γ 's ($E_\gamma \geq 1\text{ GeV}$) between 3° – 40° cones of the track selected from the $\tau(1+1)$ sample. The solid line in each plot indicates the fit and the dashed curves show the contributions from various types of particles.

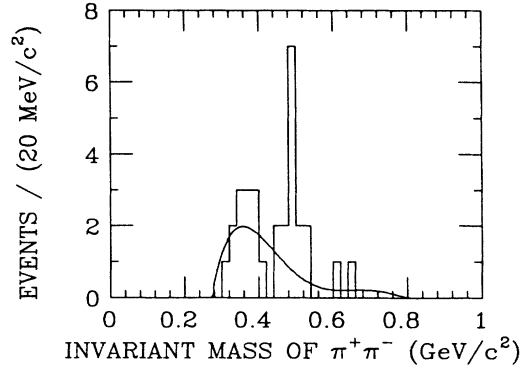


FIG. 3. The invariant mass of $\pi^+\pi^-$ in K_S^0 candidates selected by vertex criteria. The smooth curve is the background calculated by Monte Carlo simulation.

had momenta $> 2\text{ GeV}/c$ (since the expected dE/dx for kaons crosses over that expected for pions at lower momentum), and were identified as nonmuons by the muon system (so that we would not have to allow for muons in the dE/dx fitting). In addition, for $\tau(1+1)$ events both prongs were required to be identified as “nonelectrons” in order to remove the tails of the radiative Bhabha background. This selection gave 317 tracks from the $\tau(1+3)$ sample and 667 tracks from the $\tau(1+1)$ sample.

The dE/dx distribution of these tracks was then fit with three Gaussian functions, as shown in Fig. 2(a). The centroids and widths of the functions were fixed to values derived previously,¹³ leaving the relative amplitudes as the only free parameters. The fit yielded 37.0 ± 7.9 kaons.

The selection efficiency for kaons was estimated to be $(10.6\pm 0.3)\%$ by using a Monte Carlo simulation of $\tau^+\tau^-$ pair production and decay via $\tau^- \rightarrow K^- \nu_\tau$, $\tau^- \rightarrow K^{*-} \nu_\tau \rightarrow K^- \pi^0 \nu_\tau$, and $\tau^- \rightarrow K^- \pi^0 \pi^0 \nu_\tau$. The Monte Carlo simulation predicts 1.7 ± 0.9 background events, mostly due to multihadron events. Combining the background-subtracted signal (35.3 ± 8.0 kaons) with the

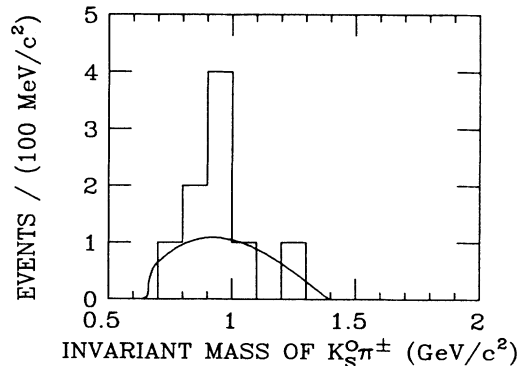


FIG. 4. The invariant mass of $K_S^0\pi^\pm$. The smooth curve is the calculated background.

TABLE V. The number of selected events and the corrections and the acceptances for each of the nine categories.

Category	No. of selected events	Background	Correction for μ - h misidentified	Trigger efficiency (%)	Selection efficiency (%)
μ -3	89.0 \pm 9.4	2.6 \pm 1.3	-5.6 \pm 1.3	96.0 \pm 0.3	17.0 \pm 0.7
e -3	108.7 \pm 10.8	4.8 \pm 2.1		96.0 \pm 0.3	18.2 \pm 0.7
h -3	196.3 \pm 14.6	21.1 \pm 3.6	+ 4.8 \pm 1.0	96.0 \pm 0.3	11.9 \pm 0.5
(μ / h)-3	162.3 \pm 13.8	10.0 \pm 2.3		96.0 \pm 0.3	6.3 \pm 0.3
Miscellaneous $\tau(1+3)$	103.7 \pm 12.5	14.3 \pm 3.4	+ 0.8 \pm 1.6	96.0 \pm 0.3	3.6 \pm 0.2
h - h	146.0 \pm 12.1	5.7 \pm 1.5	+ 7.0 \pm 1.5	67.3 \pm 2.8	9.8 \pm 0.3
e - μ	51.8 \pm 7.7		-3.4 \pm 0.9	67.8 \pm _{13.2} ^{6.7}	9.7 \pm 0.5
h - μ	151.2 \pm 12.7	1.1 \pm 0.5	-5.2 \pm 2.3	67.3 \pm 2.8	11.1 \pm 0.5
(μ / h)- h	185.0 \pm 13.6	12.7 \pm 2.9	+ 4.4 \pm 1.0	70.0 \pm 4.5	5.3 \pm 0.2

luminosity, the detection efficiency, and the theoretical cross section, the branching ratio B_K was found to be (1.6 \pm 0.4 \pm 0.2)%. The first error is statistical, and the second is the systematic error due to the uncertainty in the luminosity (5%), the dE/dx analysis (8%), and uncertainty in the relative contributions of the various modes (3%). Subtracting B_K from B_h measured previously, we obtain a $B_\pi = B(\tau^- \rightarrow \pi^- + \text{neutrals})$ of (47.0 \pm 1.2 \pm 0.9)%.

VIII. $B(\tau^- \rightarrow K^- + \pi^0 + \text{NEUTRAL PARTICLES})$

Although our π^0 reconstruction efficiency was too low to search for neutral pions associated with the kaons directly, we used the detection of high-energy photons in the single-prong decay to infer their presence. Of the 667 tracks selected previously from the $\tau(1+1)$ sample, 217 had energetic photons ($E_\gamma \geq 1$ GeV) between 3° and 40° of the track direction. The cuts were designed to reject bremsstrahlung photons while maximizing the acceptance for photons from π^0 decay. 83% of the photons were found in the HEX calorimeter, the rest were reconstructed photon pair conversions from the TPC. The dE/dx distribution for the tracks with associated photons is shown in Fig. 2(b). The resulting fit gave 8.6 \pm 3.6 kaons.

A detection efficiency of 3.5 \pm _{0.2}^{1.1}% was estimated by taking the Monte Carlo-calculated efficiency for

$\tau^- \rightarrow K^{*-} \nu_\tau \rightarrow K^- \pi^0 \nu_\tau$, and inserting a large positive systematic error to allow for up to a one-third $\tau^- \rightarrow K^- \pi^0 \pi^0 \nu_\tau$ component (which has a higher detection efficiency because of the larger number of photons). The background contamination was negligible according to the Monte Carlo simulation. Then, following the same calculation as for B_K , $B_{K\pi^0}$ was determined to be (1.2 \pm 0.5 \pm _{0.4}^{0.2})%. The first error is statistical. The second is systematic, and reflects the uncertainty in the detection efficiency (30%), the luminosity (5%), and dE/dx analysis (11%).

IX. $B(\tau^- \rightarrow K^{*-} + \text{NEUTRAL PARTICLES})$

The branching ratio B_{K^*} was measured using the three-prong decays from $\tau(1+3)$ events, where $K^{*\pm}(892) \rightarrow K_S^0 \pi^\pm \rightarrow \pi^+ \pi^- \pi^\pm$. K_S^0 candidate combinations were formed of opposite-sign tracks in the three-prong decays. A track pair was accepted as a K_S^0 candidate if the following criteria were satisfied: (1) The distance of closest approach between the tracks was ≤ 0.4 cm; (2) the momentum vector of the pair pointed within 2° of the event vertex; (3) the flight path from the event vertex was between 3 and 50 cm; (4) the angle in the K_S^0 center-of-mass system between the tracks and the direction defined by the K_S^0 momentum in the laboratory sys-

TABLE VI. Published measurements and this measurement of branching ratios B_e and B_μ . Measurements marked with a dagger used lepton universality to fix the ratio of B_e to B_μ . Also shown are the predictions from the measured τ lifetime (Ref. 14).

Collaboration	B_e	B_μ
Mark II (Ref. 19) [†]	(17.6 \pm 0.6 \pm 1.0)%	(17.1 \pm 0.6 \pm 1.0)%
PLUTO (Ref. 20)	(13.0 \pm 1.9 \pm 2.9)%	(19.4 \pm 1.6 \pm 1.7)%
TASSO (Ref. 21)	(20.4 \pm 3.0 \pm _{0.9} ^{1.4})%	(12.9 \pm 1.7 \pm _{0.5} ^{0.7})%
CELLO (Ref. 22)	(18.3 \pm 2.4 \pm 1.9)%	(17.6 \pm 2.6 \pm 2.1)%
Mark III (Ref. 23)	(18.2 \pm 0.7 \pm 0.5)%	(18.0 \pm 1.0 \pm 0.6)%
MAC (Ref. 24) [†]	(17.8 \pm 0.5)%	(17.3 \pm 0.5)%
Average	(17.9 \pm 0.4)%	(17.2 \pm 0.4)%
(Lifetime)	(18.2 \pm 1.1)%	(17.7 \pm 1.0)%
This paper	(18.4 \pm 1.2 \pm 1.0)%	(17.7 \pm 1.2 \pm 0.7)%
This paper [†]	(18.3 \pm 0.7 \pm 0.5)%	(17.8 \pm 0.7 \pm 0.5)%

TABLE VII. Published measurements and this measurement of branching ratios B_1 and B_3 .

Collaboration	B_1	B_3
Mark II (Ref. 25)	$(86 \pm 2 \pm 1)\%$	$(14 \pm 2 \pm 1)\%$
CELLO (82) (Ref. 10)	$(84.0 \pm 2.0)\%$	$(15.0 \pm 2.0)\%$
CELLO (84) (Ref. 26)	$(85.2 \pm 1.9 \pm 1.3)\%$	$(14.8 \pm 1.5 \pm 1.3)\%$
PLUTO (Ref. 20)	$(87.8 \pm 1.3 \pm 3.9)\%$	$(12.2 \pm 1.3 \pm 3.9)\%$
TASSO (Ref. 21)	$(84.7 \pm 1.1 \pm 1.3)_{-1.3}^{+1.6}\%$	$(15.3 \pm 1.1 \pm 1.3)_{-1.6}^{+1.3}\%$
TPC (Ref. 27)	$(85.2 \pm 0.9 \pm 1.5)\%$	$(14.8 \pm 0.9 \pm 1.5)\%$
MAC (Ref. 28)	$(86.7 \pm 0.3 \pm 0.6)\%$	$(13.3 \pm 0.3 \pm 0.6)\%$
HRS (Ref. 29)	$(86.9 \pm 0.2 \pm 0.3)\%$	$(13.0 \pm 0.2 \pm 0.3)\%$
JADE (Ref. 11)	$(86.1 \pm 0.5 \pm 0.9)\%$	$(13.6 \pm 0.5 \pm 0.8)\%$
DELCO (Ref. 30)	$(87.9 \pm 0.5 \pm 1.2)\%$	$(12.1 \pm 0.5 \pm 1.2)\%$
Average	$(86.8 \pm 0.3)\%$	$(13.1 \pm 0.3)\%$
This paper	$(84.7 \pm 0.8 \pm 0.6)\%$	$(15.1 \pm 0.8 \pm 0.6)\%$

tem was $> 11.5^\circ$.

The invariant mass of the 28 K_S^0 candidates which passed these criteria are shown in Fig. 3, along with the background expected according to Monte Carlo calculations normalized to 77 pb^{-1} . The 13 K_S^0 candidates in the invariant-mass region of $0.45\text{--}0.55 \text{ GeV}/c^2$, with an estimated background of 3.6 ± 0.5 , were then selected to carry out the $K^{*\pm}$ search.

Figure 4 shows the invariant-mass distribution of the K_S^0 and remaining track combination, with the requirement that the momentum resolutions of the K_S^0 and the other tracks had $\delta P/P \leq 25\%$. The Monte Carlo-estimated background is also shown. A fit to this distribution using the known $K^{*\pm}$ mass and width, our calculated detector resolution, and the Monte Carlo background yield $4.6 \pm 2.9 K^{*\pm}$. The $K^{*\pm}$ detection efficiency was estimated to be $(6.9 \pm 0.4)\%$. The resulting branching ratio is $B_{K^*} = (1.4 \pm 0.9 \pm 0.3)\%$, where the systematic error is dominated by uncertainty in the background estimation.

X. DISCUSSION

Our measured B_e of $(18.3 \pm 0.9)\%$ (derived using lepton universality and adding statistical and systematic errors in quadrature) is very close to the current world average of $(17.9 \pm 0.4)\%$ (Table VI), and the predicted value of

$(18.2 \pm 1.1)\%$ found using the standard model and the measured τ lifetime of $(2.90 \pm 0.17) \times 10^{-13} \text{ sec}$ (Ref. 14). However, our measured B_3 of $(15.1 \pm 1.0)\%$ is higher than the current world average of $(13.1 \pm 0.3)\%$ (Table VII). If we use our measurement of B_e and B_3 to do a calculation similar to Ref. 1, the excess in the one-prong decay mode is reduced because of our lower B_1 measurement and because limits on some contributions to the one-prong mode are set from the measured three-prong rate, which is higher in our data. However, including our results in the world averages does not significantly alter the discrepancy.

Our measurement of $B(\tau^- \rightarrow K^- + \text{neutral particles}) = (1.6 \pm 0.4)\%$ agrees with the DELCO Collaboration¹⁵ measurement of $(1.7 \pm 0.3)\%$. This rate is consistent with the sum of theoretically estimated contributions to this single-prong mode of 0.7, 0.4, 0.3, and 0.2% from $\tau^- \rightarrow K^- \nu_\tau$, $\tau^- \rightarrow K^{*-} \nu_\tau$, $\tau^- \rightarrow K^- K^0 \nu_\tau$, and $\tau^- \rightarrow \rho(1600) \nu_\tau \rightarrow K^- K^0 \pi^0 \nu_\tau$, respectively; however, the estimates for the last two modes are rather uncertain.¹ Our measurement of the τ branching ratio to $(K^- \pi^0 + \text{neutral particles})$ of $(1.2 \pm 0.6)\%$ can be compared to 1.0 ± 0.4 obtained by taking the difference between the inclusive K^- branching ratio above and measurements of $B(\tau^- \rightarrow K^- \nu_\tau)$ of $(1.3 \pm 0.5)\%$ and $(0.59 \pm 0.18)\%$ by the Mark II (Ref. 16) and DELCO (Ref. 15) Collaborations. The theoretically estimated contributions from the four exclusive modes above are 0.0, 0.4, 0.1, and 0.2%, respectively, in reasonable agreement with our result. Our mea-

TABLE VIII. Our measurements of τ branching ratios for modes involving kaons, comparable published measurements, and theoretical estimates.

Collaboration	$B(\tau^\pm \rightarrow K^\pm + \text{neutral particles})$	$B(\tau^\pm \rightarrow K^\pm \nu_\tau)$	$B(\tau^\pm \rightarrow K^\pm \pi^0 + \text{neutral particles})$	$B(\tau^\pm \rightarrow K^{*\pm} + \text{neutral particles})$
Mark II (82) (Refs. 16 and 17)		$(1.3 \pm 0.5)\%$		$(1.7 \pm 0.7)\%$
Mark II (86) (Ref. 18)				$(1.3 \pm 0.3 \pm 0.3)\%$
DELCO (Ref. 15)	$(1.71 \pm 0.29)\%$	$(0.59 \pm 0.18)\%$		
This paper	$(1.6 \pm 0.4 \pm 0.2)_{-0.2}^{+0.5}\%$		$(1.2 \pm 0.5 \pm 0.3)_{-0.4}^{+0.3}\%$	$(1.4 \pm 0.9)\%$
Theory	1.6%	0.7% ^a	0.7%	1.4%

^aEstimate does not include possible contribution from $\tau^\pm \rightarrow K^\pm K_L^0 \nu_\tau$ with undetected K_L^0 .

surement of the inclusive branching ratio to K^{*-} of $(1.4 \pm 0.9)\%$ can be compared to the results of Mark II at SPEAR (Ref. 17) and at SLAC PEP (Ref. 18) Collaborations of $B(\tau^- \rightarrow K^{*-} \nu_\tau)$ equal to $(1.7 \pm 0.7)\%$ and $(1.3 \pm 0.4)\%$, and to expected contributions from the four exclusive modes above of 0.0, 1.2., 0.0, and 0.2 %. These results are summarized in Table VIII.

In summary, we have used the particle-identification abilities of the TPC facility to measure decay branching ratios of the τ lepton to electrons, muons, charged pions, kaons, and the $K^{*-}(890)$ resonance. The results agree

with other experiments and with expectations from the standard model.

ACKNOWLEDGMENTS

We acknowledge the efforts of the PEP staff, and of the engineers, programmers and technicians of the collaborating institutions who made this work possible. This work was supported in part by the Department of Energy, the National Science Foundation, the Joint Japan-U.S. Collaboration in High Energy Physics, and the Foundation for Fundamental Research on Matter in The Netherlands.

¹F. J. Gilman and S. H. Rhie, Phys. Rev. D 31, 1066 (1985).

²H. Aihara *et al.*, IEEE Trans. Nucl. Sci. **NS-30**, 63 (1983); **NS-30**, 67 (1983); **NS-30**, 76 (1983); **NS-30**, 117 (1983); **NS-30**, 153 (1983); **NS-30**, 162 (1983).

³M. Ronan *et al.*, IEEE Trans. Nucl. Sci. **NS-29**, 427 (1982).

⁴F. A. Berends and R. Kleiss, Nucl. Phys. **B177**, 237 (1981).

⁵T. Sjöstrand, Comput. Phys. Commun. **27**, 243 (1982).

⁶Particle Data Group, C. G. Wohl *et al.*, Rev. Mod. Phys. **56**, S1 (1984).

⁷R. F. van Daalen Wetters, Ph.D. thesis, UCLA, 1985.

⁸X-Q. Lu, Ph.D. thesis, The Johns Hopkins University, 1986.

⁹P. R. Burchat *et al.*, Phys. Rev. Lett. **54**, 2489 (1985); I. Beltrami *et al.*, *ibid.* **54**, 1775 (1985).

¹⁰H. J. Behrend *et al.*, Phys. Lett. **B114**, 282 (1982).

¹¹W. Bartel *et al.*, Phys. Lett. **B161**, 188 (1985).

¹²The correlation coefficients for (B_e, B_μ) , (B_e, B_h) , and (B_h, B_μ) are -0.29 , -0.46 , and -0.52 .

¹³M. Shapiro, Ph.D. thesis, Report No. LBL-18820, 1984; W-M. Zhang, Ph.D. thesis, The Johns Hopkins University, 1986. Briefly, the dE/dx resolution and scale were found using hadrons from the one-photon annihilation sample and muons identified by the muon system in the $\tau\tau$ sample.

¹⁴See the review by E. H. Thorndike, in *Proceedings of the 1985*

International Symposium on Leptons and Photon Interactions at High Energies, Kyoto, Japan, edited by M. Konuma and K. Takahashi (Research Institute for Fundamental Research, Kyoto University, Kyoto, 1986).

¹⁵G. B. Mills *et al.*, Phys. Rev. Lett. **52**, 1944 (1984).

¹⁶C. A. Blocker *et al.*, Phys. Rev. Lett. **48**, 1586 (1982).

¹⁷J. M. Dorfan *et al.*, Phys. Rev. Lett. **46**, 215 (1981).

¹⁸J. M. Yelton *et al.*, Phys. Rev. Lett. **56**, 812 (1986).

¹⁹C. A. Blocker *et al.*, Phys. Lett. **109B**, 119 (1982).

²⁰C. Berger *et al.*, Z. Phys. C **28**, 1 (1985).

²¹M. Althoff *et al.*, Z. Phys. C **26**, 521 (1985).

²²H. J. Behrend *et al.*, Phys. Lett. **127B**, 270 (1983).

²³R. M. Baltrusaitis *et al.*, Phys. Rev. Lett. **55**, 1842 (1985).

²⁴W. W. Ash *et al.*, Phys. Rev. Lett. **55**, 2118 (1985).

²⁵C. A. Blocker *et al.*, Phys. Rev. Lett. **49**, 1369 (1982).

²⁶H. J. Behrend *et al.*, Z. Phys. C **23**, 103 (1984).

²⁷H. Aihara *et al.*, Phys. Rev. D **30**, 2436 (1984). The data used in this reference are a subsample of the data used for the current analysis.

²⁸E. Fernandez *et al.*, Phys. Rev. Lett. **54**, 1624 (1985).

²⁹C. Akerlof *et al.*, Phys. Rev. Lett. **55**, 570 (1985).

³⁰W. Ruckstuhl *et al.*, Phys. Rev. Lett. **56**, 2132 (1986).